ELSEVIER

Polymer 40 (1999) 3001–3011

polymer

Electron microprobe analysis as a novel technique to study the interface between thermoset and thermoplastic polymers

Hideko T. Oyama[a,*], T.N. Solberg[b], J.P. Wightman[a]

[a]*Department of Chemistry, NSF Science and Technology Center for High Performance Polymeric Adhesives and Composites, Virginia Polytechnic Institute & State University, Blacksburg, VA 24061-0212, USA*
[b]*Department of Geological Sciences, Virginia Polytechnic Institute & State University, Blacksburg, VA 24061-0420, USA*

Received 12 September 1997; accepted 24 February 1998

Abstract

Bilayer films between thermoset epoxy and thermoplastic poly(vinylpyrrolidone) (PVP) were prepared by casting a stoichiometric mixture of the uncured diglycidyl ether of bisphenol A epoxy (DGEBA) and 4,4′-diaminodiphenylsulfone (DDS) on a PVP film and then curing the system in a two-step process under an inert gas atmosphere. The resultant interface was analyzed by electron microprobe analysis (EMP). The EMP results demonstrated that the interface formation was predominantly controlled in the initial cure stage, and that the diffusion at the interface was suppressed significantly after the epoxy formed the network structure. New EMP techniques were developed to analyze the polymer–polymer interface and to obtain not only the concentration profile but also the image of the interface. The limit of the resolution was 1.6 μm under the experimental conditions employed in this study.

Keywords: Interface/interphase; Concentration profile; Electron microprobe analysis

1. Introduction

It is widely known that the interface region plays an important role in numerous areas such as polymer blends, adhesives, and composites [1–3]. There have been many techniques described in the literature to study the polymer–polymer interface; for example, microscopic methods such as SEM [4] and TEM [5] combined with analytical tools, ellipsometry [6], neutron scattering [7], secondary ion mass spectroscopy [8,9], vibrational spectroscopic methods such as i.r. [10,11] and Raman [12] spectroscopy, and ion-beam analysis such as forward recoil spectroscopy [13,14] and Rutherford backscattering [14,15]. These techniques have been mainly applied to the interface formed between two thermoplastic polymers, where most interfaces were much thinner than a micrometer.

Although composites and adhesives are commonly prepared using a thermoset prepolymer, so far the interface between thermoset and thermoplastic polymers has hardly been studied. When a bilayer film of thermoset and thermoplastic polymers was prepared from an uncured thermoset pre-polymer in our previous study [16], it was found that the interfacial thickness was of the order of 10 μm. Since the interfacial thickness was significantly larger than that of conventional systems, electron microprobe analysis (EMP) was employed for the first time to characterize the polymer–polymer interface.

In EMP, the measured radiation is a characteristic X-ray generated as a result of transitions between inner atomic electron energy levels, which are stimulated by electron excitation [17]. The X-ray spectrum is recorded in either of two modes, giving rise to the techniques of ‘wavelength-dispersive spectroscopy’ (WDS) or ‘energy-dispersive spectroscopy’ (EDS). From the wavelength (or photon energy) and intensity of the lines in the X-ray spectrum, the existing elements can be identified and their concentrations can be estimated. The use of a finely focused electron beam enables a very small selected area to be analyzed. Here, the electron energy has to be chosen higher than the so-called ‘critical excitation energy’, which is the minimum energy necessary to generate the characteristic X-ray. The incident electrons typically have a kinetic energy of 10–30 keV and penetrate the sample to a depth of the order of 1 μm, spreading out laterally to a similar distance. The actual analytical

* Corresponding author.

0032-3861/99/$ - see front matter
PII: S0032-3861(98)00192-X

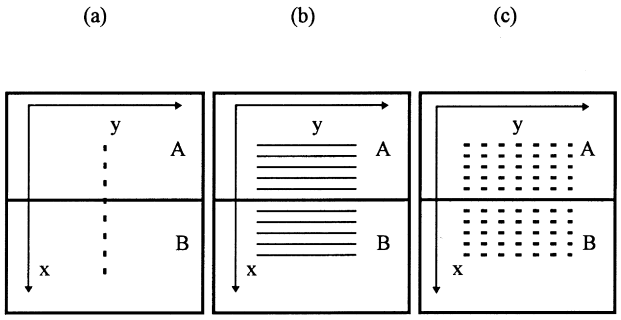

Fig. 1. Three different modes developed for electron microprobe analysis: (a) a spot step mode ⇒ $I(x)$; (b) a line step mode ⇒ $I(x)$; (c) a mapping mode ⇒ $I(x,y)$.

resolution under the experimental conditions chosen in the present study will be discussed later.

EDS has some advantages over WDS. EDS records the whole X-ray spectrum simultaneously, whereas WDS does not. A recent remarkable advancement in EDS enables the measurement of light elements. However, the resolving power of EDS is substantially inferior to that of WDS.

WDS utilizes a diffracting crystal which acts as a monochromator, selecting one wavelength at a time, depending on the angle of incidence of the X-rays. Most instruments have two or more spectrometers with crystals covering different wavelength ranges. The sample chamber is evacuated (typically 10^{-3} Pa or less) in order to prevent absorption of the X-rays in air.

In the present work, WDS was chosen as a detector because of the high accuracy of this technique. The CAMECA SX-50 spectrometer could monitor four signals in different directions simultaneously. The recent development of a synthetic multilayer crystal enabled the measurement of light elements such as nitrogen successfully, although the measurement of such light elements is still more difficult than heavier elements.

In the first report, the interface region was analyzed in 'a spot step mode', in which the interface region was scanned perpendicular to the interface direction at 2 μm intervals with an electron beam possessing a 2 μm diameter [16]. This method successfully provided a concentration profile of $I(x)$, the intensity at distance, x, measured perpendicular to the interface direction. However, the electron beam damaged the sample surface as observed by the appearance of a trace of the scanned line across the interface.

In order to minimize sample damage, 'a line step mode' was developed in the present study. In the line step mode, the intensity of an emitted characteristic X-ray at a certain distance away from the interface was measured again, but this time the signal was collected not from a single spot, but from a line of 1 μm width and 30–100 μm length rastered precisely parallel to the interface direction. The lines scanned parallel to the interface direction were successively moved 1 μm stepwise perpendicular to the interface direction, x. The total length of the step scan was 150 μm (the scanned distance perpendicular to the interface). Thus, the $I(x)$ was obtained as an averaged intensity at different y values, in which y is a distance parallel to the interface direction. This method successfully reduced the sample damage because the electron beam did not stay at one spot during collection of the signal.

Another method, 'a mapping mode', was also applied to the polymer–polymer interface in this study. The concentration of each element present in the interphase was determined in two dimensions. In other words, the area to be analyzed was divided by 256 × 256 pixels (or by 512 × 512 pixels) and the intensity was measured at each pixel, $I(x,y)$. A suitable magnification was selected for each system and the corresponding scale in μm/pixel was calculated. The $I(x,y)$ values provided both a two-dimensional interface image and a concentration profile by averaging the intensity at different y values. These three modes developed for the EMP measurements are illustrated in Fig. 1.

The line step mode was very useful for measuring a concentration profile with a rather short data acquisition time. However, special care was needed to align the scanned line exactly parallel to the interface, otherwise the measurement would average concentrations at different distances from the interface. On the other hand, the mapping mode was a very useful technique to obtain a visual interface image, in which the interface region could be imaged as a color gradient (or a gray scale), in which the color corresponded to the concentration of a given element present at the interface. However, the mapping mode required a long data acquisition time (at least several hours per image) in order to obtain good visualization. From the resultant image, the concentration profile could be calculated using a computer program. If the mapping mode was used not to measure the image, but only to get a concentration profile, the data acquisition time could be set much shorter. The mapping mode provided data points at submicron intervals, which were finer than those obtained by the step mode. In the present study, these new methods for EMP measurement proved to be very powerful in order to study the polymer–polymer interface, as described below.

In the previous work, the interface of a bilayer film prepared from poly(vinylpyrrolidone) (PVP) and the mixture of non-brominated and brominated epoxies, Epoxy^{*Br}/PVP, was analyzed [16]. The effects of the cure cycle and molecular weight of PVP were reported. It was demonstrated for the first time that the stoichiometry between epoxy and a curing agent was not always preserved in the interphase, in which the curing agent tended to move preferentially towards the thermoplastic PVP phase compared to the epoxy. This tendency became more significant with an increase in the interfacial thickness. Since EMP was shown to be effective for monitoring a light element present in the system, a bilayer film prepared from non-brominated epoxy and PVP, Epoxy/PVP, was studied here. Attention was placed at examining in detail the interface structure at the postcure stage.

2. Experimental

2.1. Materials

Two types of epoxy resin, based on the diglycidyl ether of bisphenol A epoxy, were used as the thermoset pre-polymers. One was a non-brominated conventional epoxy, DER331 manufactured by Dow Chemical Company with an epoxide equivalent weight (EEW) of 187.4. The other was a tetra-brominated epoxy, DER542 manufactured by the same company with an EEW of 333. The detailed structures were provided in the previous paper [16].

Poly(vinylpyrrolidone) (PVP) with a viscosity average molecular weight of 1 100 000 [18], PVP(K90), was obtained from the BASF Corporation as a gift. The PVP film was prepared by casting a solution of PVP in a methanol/water mixture (1/1 by volume) and drying it very slowly at room temperature (3–4 weeks).

In order to remove not only moisture but also internal stresses caused during film preparation, the PVP films were heated once to 220°C for 0.5 h under vacuum and cooled down very slowly, just prior to casting the epoxy on their upper surface. Meanwhile, the epoxy pre-polymer was heated at 110°C with a stirrer under vacuum for 1 h in order to remove low boiling impurities including water, and then a stoichiometric amount of a curing agent, 4,4′-diaminodiphenylsulfone (DDS), was added to the epoxy. When the DDS was dissolved completely in the epoxy at 110–115°C under vacuum, the mixture was cast on the dried PVP film. It was confirmed by infrared spectroscopy that the epoxy mixture prepared in this way had not initiated the cure reaction at this stage.

The bilayer films of epoxy and PVP were obtained by heating the system at two sets of cure conditions under an inert gas atmosphere (nitrogen or argon); one was 130°C for 4 h and then 220°C for different times and the other was 170°C for 2 h and then 220°C for different times. The sample temperature during the cure reaction was controlled as precisely as possible ($< \pm 1.0$°C). The bilayer films prepared from DER331 and PVP(K90) were denoted as Epoxy/PVP. The data on characterization of the Epoxy/PVP interface were compared with those of the bilayer films prepared from (1/1 by wt.) (DER331 + DER542) and PVP reported in the previous paper [16], which were denoted as Epoxy^{*Br}/PVP.

In order to examine whether diffusion can occur at the interface between the precured epoxy and a thermoplastic linear polymer, bilayer films of the cured epoxy and PVP were prepared separately. First, a stoichiometric mixture of DER331 and DDS was cured at 170°C (2 h) + 220°C (2 h) in an inert gas atmosphere and then the PVP solution of a methanol/water mixture (1/1 by volume) was cast on the epoxy surface. After the PVP film dried completely, the bilayer film was heated at 220°C for various times and used for the EMP measurement.

2.2. Analysis

The glass transition temperatures, T_g, of PVP and epoxy cured under different conditions were measured with a differential scanning calorimeter (Perkin-Elmer DSC-7) under nitrogen gas at a heating rate of 10°C/min.

Electron microprobe analysis (CAMECA SX-50) was performed both in a line step scan mode and in a mapping mode. The cross-section of the bilayer film was coated with carbon (25 nm) prior to the measurements in order to make it conductive and to protect the polymers from beam damage to some extent. The data were acquired by monitoring the sulfur signal from DDS and the nitrogen signal from both DDS and PVP. For the bilayer films prepared using the brominated epoxy, the bromine signal was also used as a probe during the scan across the interface [16].

WDS was employed as a technique using a pentaerythritol crystal (PET) to measure the K_α line of sulfur, a synthetic multilayer crystal made of silicon and tungsten (PC1) to monitor the K_α line of nitrogen, and a thallium acid phthalate crystal (TAP), $C_8H_5O_4Tl$, to measure the L_α line of bromine [17].

In the line step mode, the accelerating voltage was set to 10 kV, the current was 10 nA, and the beam spot size was 1 μm. The data at a certain distance from the interface were acquired by scanning 30–100 μm lines, which were aligned precisely parallel to the interface. The lines scanned parallel to the interface direction were moved 1 μm stepwise perpendicular to the interface direction in order to obtain the compositional change at different positions in the interphase. The total length of the step scan was 150 μm (the scanned distance perpendicular to the interface). The data acquisition time was set to 20 ms/line.

On the other hand, in the mapping mode the accelerating voltage and the current were set to be the same, however, the resolution was chosen to be 256 × 256 pixels with 0.333 μm/pixel (Figs. 4 and 5) and 512 × 512 pixels with 0.0954 μm/pixel (Fig. 10). The acquisition time was 50 ns/pixel. The electron beam was narrowed to a submicron size. One beam scan took 2 h and at least 10 scans were averaged in order to obtain one image. Images were processed by a photographic computer program, IMAGE, distributed by National Institute of Health, from which the concentration profiles were obtained.

3. Results and discussion

3.1. Increase in glass transition temperature of the epoxy upon curing

A stoichiometric mixture of DER331 and DDS was heated at different conditions in order to monitor the change of the epoxy phase during the bilayer film formation. The glass transition temperature (T_g) of the epoxy itself was

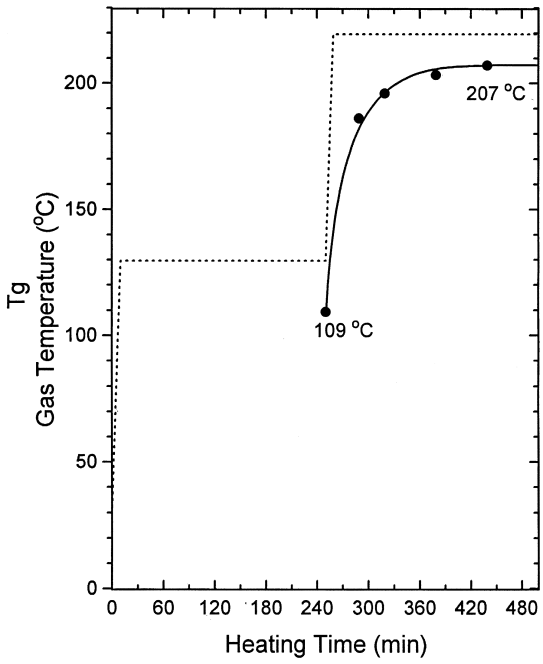

Fig. 2. Increase in glass transition temperature, T_g (●) of the epoxy cured at 130°C + 220°C. The dotted line shows the temperature of argon used to purge the furnace. The heating time indicates the total heating time. In the first 4 h heating was at 130°C and in the next 3 h heating was at 220°C. The heating rate was set to 10°C/min.

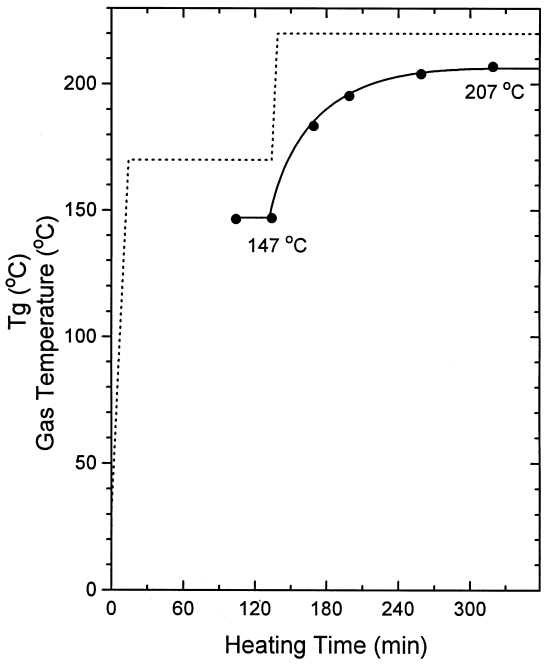

Fig. 3. Increase in glass transition temperature, T_g (●) of the epoxy upon the cure reaction of 170°C + 220°C. The dotted line shows the temperature of argon used to purge the furnace. The heating time indicates the total heating time. In the first 2 h heating was at 170°C and in the next 3 h heating was at 220°C. The heating rate was set to 10°C/min.

measured by differential scanning calorimetry (d.s.c.). Fig. 2 shows the results for the T_g of the epoxy, which was cured at 130°C (4 h) + 220°C (various times up to 3 h). The dashed line indicates the temperature of argon used to purge the furnace in order to cure the epoxy. The data showed that the glass transition temperature was still as low as 109°C at the end of the first cure step; however, it reached the final T_g by additional heating at 220°C for 2 h. Fig. 3 shows the corresponding results for the T_g of the epoxy, which was cured at 170°C (2 h) + 220°C (various times up to 3 h). It shows that at the end of the first cure step, the T_g was 147°C and that further heating at 220°C brought the epoxy system to a final T_g in 2 h, as observed in Fig. 2. The postcure temperature of 220°C was selected to be higher than the final T_g of the epoxy phase, 207°C, in order to complete the cure reaction.

Simpson and Bidstrup reported rheological and dielectric changes during the cure reaction between DGEBA and DDS, in which their data on T_g showed a good agreement with our data [19]. The cure conversion of epoxide group at the end of the initial cure of 130°C (4 h) was roughly estimated at 0.83 and that at the end of the initial cure of 170°C (2 h) was 0.91 from their results. Min et al. also examined the cure reaction between DGEBA and DDS using d.s.c. and near infrared spectroscopy [20,21]. The conversion of epoxide group was roughly estimated at 0.8 at 130°C (4 h), which showed a reasonable agreement with the estimate based on Simpson and Bidstrup's paper. Cure conversions of the primary amine and the secondary amine, corresponded to approximately 1 and 0.4, respectively, at 130°C (4 h). Since the gel point of the present DGEBA–DDS system was reported to be 0.58 of the epoxide conversion [19], these results indicate that at the end of the initial cure stage of both 130°C (4 h) and 170°C (2 h) in our experiment, the cure reaction progressed much further than the gel point.

Min and co-workers proposed a model derived on the assumption that the T_g had individual linear relationships with the degree of conversion of the two reactions, i.e. linear polymerization and crosslinking, which agreed well with the experimental data [20]. The observed T_g was expressed by the following equation

$$T_g = T_{g0} + \alpha_L[(T_{g\infty})_L - T_{g0}] + \alpha_C[T_{g\infty} - (T_{g\infty})_L]$$

where T_{g0}, $T_{g\infty}$, and $(T_{g\infty})_L$ are the T_g of the unreacted monomer mixture, the maximum T_g of the fully cured epoxy, and the limiting T_g of a linear polymer of infinite molecular weight, respectively. The α_L and α_C are the conversions of the linear polymerization and the crosslinking reactions, respectively. Their results showed that $(T_{g\infty})_L$ was 34°C and $T_{g\infty}$ was 205°C, in which the maximum T_g increase by linear polymerization was only 40°C, whereas that by the crosslinking reaction was 171°C, demonstrating the important contribution of the crosslinking reaction to the T_g.

Furthermore, it was reported that the relationship between T_g and the cure conversion was independent of cure temperature in the stoichiometric DGEBA–DDS system [19]. Similar results were observed in other epoxy systems [22]. This implies that either the molecular structure of the

epoxies cured at different temperatures is the same or that the structural differences do not have a significant effect on the T_g.

Lastly, from the previous study [16] the T_g of the present PVP with the viscosity average molecular weight (M_v) of 1 100 000 was estimated to be 177°C, whereas that with M_v of 9200 was as low as 106°C.

3.2. Epoxy/PVP bilayer film

3.2.1. Interface image

The interfaces of the Epoxy/PVP bilayer films prepared at 130°C (4 h) + 220°C (2 h), and at 170°C (2 h) + 220°C (2 h) were investigated by EMP in the mapping mode, as shown in Fig. 4 and Fig. 5, respectively. Fig. 4(a) and Fig. 5(a) show the interface image monitored by the sulfur signal in an 85 × 85 μm dimension, and Fig. 4(b) and Fig. 5(b) show that measured by the nitrogen signal at the same location. In these images the left phase was the epoxy phase and the right phase was the PVP phase. Both images indicated that the interface was quite straight. In principle, the intensity of the signal at any point corresponds to the concentration of the element present. However, strictly speaking this applies to the contrast between two phases in a single image. For comparison between different images sometimes intensity differences can arise for two reasons. First, intensity is enhanced with an increase in the data acquisition time. Second, the intensity of the observed signals is also affected by the exact positioning and alignment of the sample with respect to the detector. Therefore, in order to minimize these effects, the samples were carefully set as horizontally as possible in the analysis chamber at the same height and the measurements were performed using the same experimental conditions. In Figs. 4 and 5, the gradient of the concentration is given by different colors; yellow > pink > blue > black from the higher concentration to the lower concentration. The epoxy phase, which contained sulfur from the curing agent, DDS, appears as a yellow

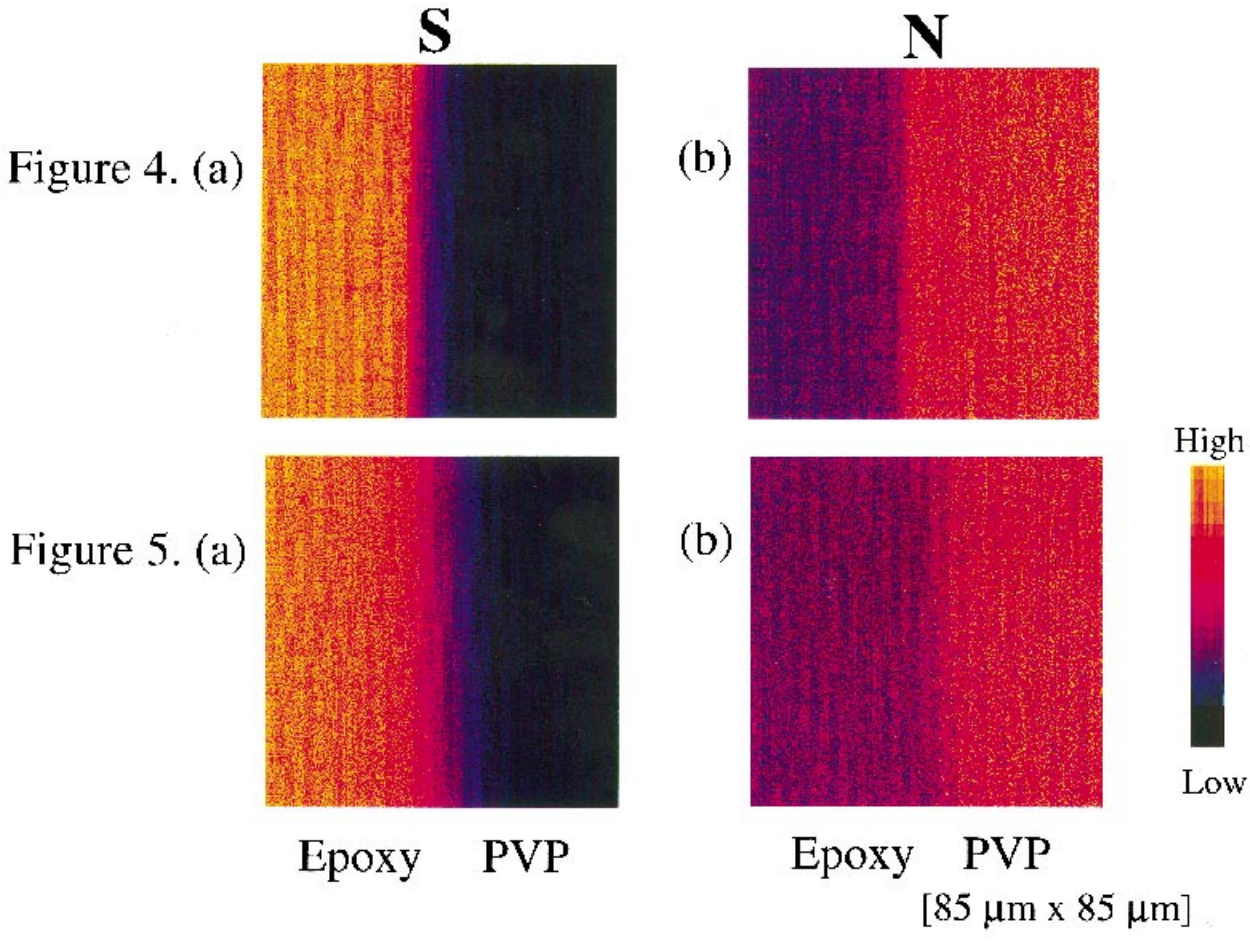

Figure 4. (a)

Figure 5. (a)

Fig. 4. Interface image of the Epoxy/PVP cured at 130°C (4 h) + 220°C (2 h) measured by the mapping mode of the EMP: (a) monitored by the sulfur signal; (b) monitored by the nitrogen signal.

Fig. 5. Interface image of the Epoxy/PVP cured at 170°C (2 h) + 220°C (2 h) measured by the mapping mode of the EMP: (a) monitored by the sulfur signal; (b) monitored by the nitrogen signal.

region with a high concentration, whereas the PVP phase with no sulfur, appears to be a black region with a low concentration. The background measurement was omitted here because it was not necessary in order to obtain a normalized concentration profile at the interface. On the other hand, in Fig. 4(b) and Fig. 5(b), the PVP phase, which contained a higher nitrogen concentration compared to the curing agent in the epoxy phase, appears as a yellowish region and the epoxy phase with a lower nitrogen concentration appears as a bluish region. Since three spectrometers for the sulfur signal and one spectrometer for the nitrogen signal were used during the EMP measurements, the sulfur image obtained by averaging more scans (30 scans for S and 10 scans for N) showed a much clearer contrast between the two phases. In addition, the nitrogen was contained in both phases, which probably contributed to a reduction of the contrast.

The change in color at the interphase in both Fig. 4(a) and Fig. 4(b) was more abrupt than that in Fig. 5(a) and Fig. 5(b) with a much narrower diffusion range at the interface. Thus, the comparison of the interface images between Figs. 4 and 5 clearly showed that the bilayer film prepared at 170°C (2 h) + 220°C (2 h) resulted in a thicker interphase compared to that prepared at 130°C (4 h) + 220°C (2 h). To our knowledge, these images are the first to show the polymer–polymer interface measured by EMP.

3.2.2. Concentration profile of the Epoxy/PVP

Since the interfacial images were composed of data points making X-ray intensity at each pixel proportional to the concentration of the monitored element, normalized concentration profiles at the interface were obtained from the images. Using the raw data of the nitrogen signal, the contributions from DDS and from PVP to the total nitrogen signal were separated by calculation based on the following assumptions [16]: first, the observed nitrogen signal in the epoxy phase came only from DDS; second, the change of the nitrogen signal originating from DDS in the interphase was the same as that of the sulfur signal; and third, the observed nitrogen signal of the PVP phase came from only PVP. This is in agreement with the individual structure of the components.

The normalized concentration profiles for PVP and DDS at the interface obtained from the interface image given in Fig. 4 are shown in Fig. 6 and characterize the Epoxy/PVP interface prepared at 130°C (4 h) + 220°C (2 h). This figure also includes the calculated concentration profile of the overall epoxy, obtained from the complement of the PVP profile, assuming that the reduction of the PVP concentration at the interface is due to the intrusion of the epoxy phase. The concentration profile of each species was quite symmetrical and continuous. The difference in the diffusion front position between DDS and the epoxy at 0.5 of their normalized concentrations was as small as 0.8 μm. Here the DDS profile moved slightly toward the PVP phase compared to the epoxy profile. The dotted lines indicate a fitting by the error function.

Similarly, Fig. 7 shows the concentration profiles of the Epoxy/PVP interface cured at 170°C (2 h) + 220°C (2 h). The region where the concentration gradients of the species were observed was larger than that for the Epoxy/PVP cured at 130°C (4 h) + 220°C (2 h), shown in Fig. 6. The profiles of the DDS and that calculated for the epoxy almost overlapped. The difference in the diffusion front position between DDS and the epoxy at 0.5 of their normalized concentrations was estimated as 0.9 μm.

The results on the interface of other systems cured at 130°C (4 h) + 220°C (various times) and at 170°C (2 h) +

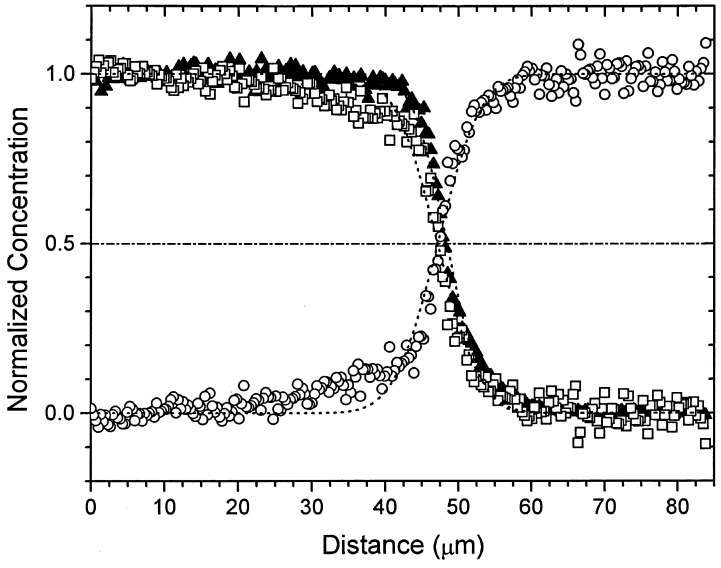

Fig. 6. Normalized concentration profiles of the Epoxy/PVP interface cured at 130°C (4 h) + 220°C (2 h). (○) PVP; (▲) DDS; (□) Epoxy (calculated).

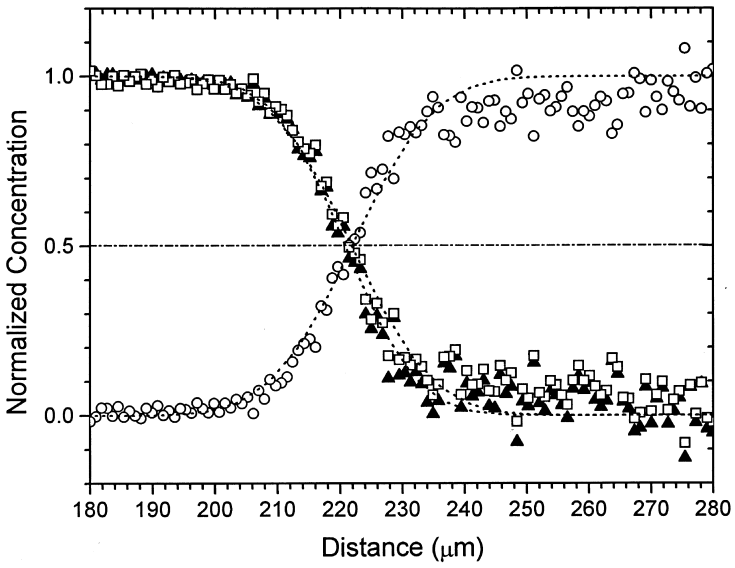

Fig. 7. Normalized concentration profiles of the Epoxy/PVP interface cured at 170°C (2 h) + 220°C (2 h). (○) PVP; (▲) DDS; (□) Epoxy (calculated).

220°C (various times) are not shown here. The data obtained by the line step mode were analyzed to calculate the interfacial thickness, which will be presented next.

3.2.3. Interfacial thickness of the Epoxy/PVP

The interfacial thickness was calculated from the concentration profiles obtained by the EMP measurements, following the method used in the previous paper [16,23]. Since the shape of the concentration profile was symmetrical, each profile was fit to the error function and then the interfacial thickness was estimated. Fig. 8 shows the change in the interfacial thickness during the bilayer film formation prepared at 130°C (4 h) + 220°C (various times). The heating time on the *x*-axis corresponds to the value shown in Fig. 2, which indicates the total heating time. In order to analyze the interface using EMP, a sample has to be solidified so that only bilayer film samples cured until the last stage could be characterized. Fig. 8 indicated that the interface structure did not change much at the postcure temperature of 220°C, even though the T_g of the epoxy phase was still increasing by the additional heating at 220°C. It clearly indicated that the interface was mostly formed at the initial cure stage. The final interfacial thickness of PVP and DDS of the Epoxy/PVP prepared at 130°C (4 h) + 220°C was 11.9 and 9.4 μm, respectively. The difference in the diffusion front position of the concentration profiles for DDS and the calculated overall epoxy phase was estimated to be 1.0 μm on average at 0.5 of their normalized concentrations.

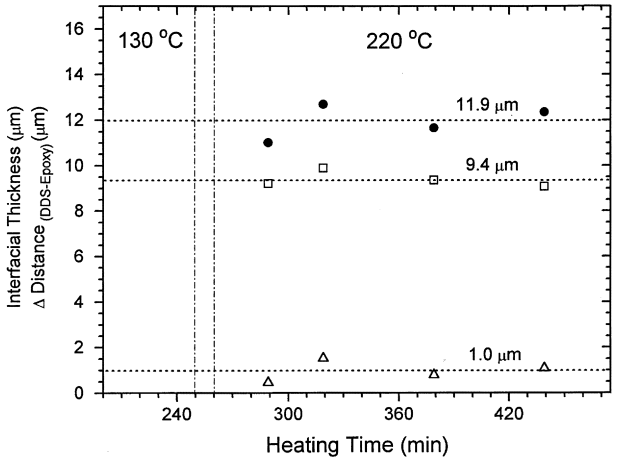

Fig. 8. Change in the interface structure of the Epoxy/PVP during the cure at (130°C (4 h) + 220°C (various times)). (●) PVP; (□) DDS; (△) ΔDistance$_{(DDS\text{-}Epoxy)}$.

In a similar manner, Fig. 9 shows the change in the interfacial thickness of the Epoxy/PVP during the reaction of 170°C (2 h) + 220°C (various times). The final interfacial thickness of PVP and DDS was 25.6 and 22.6 μm, respectively, both of which were much larger than those for the Epoxy/PVP prepared at 130°C (4 h) + 220°C. The bilayer film did not change the structure after heating at 170°C (2 h) + 220°C (0.5 h). The difference in the diffusion front position between DDS and the overall epoxy estimated from their concentration profiles was as small as 0.6 μm on average at the postcure stage.

Thus, the above results indicate that the interface between Epoxy and PVP was mostly formed at the initial cure stage, in which diffusion before the gel point is reached would be most important. This implies that the diffusion at the initial cure stage where the PVP bulk was in a glassy state and the epoxy transformed from a liquid state to a rubbery state was much faster compared to that at the postcure stage where both bulks of PVP and crosslinked epoxy were in a rubbery state. Since it was observed that PVP and the epoxy had good miscibility [16], the interface formation might also be controlled by a solution process between the two phases.

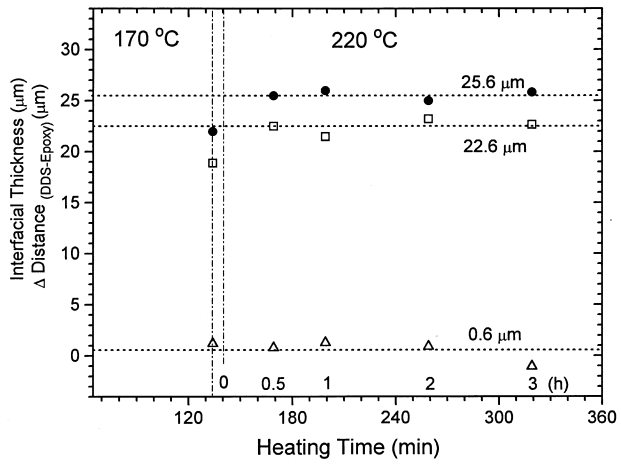

Fig. 9. Change in the interface structure of the Epoxy/PVP during the cure at 170°C (2 h) + 220°C (various times). (●) PVP; (□) DDS; (△) $\Delta Distance_{(DDS\text{-}Epoxy)}$.

3.2.4. Comparison between Epoxy/PVP and Epoxy^{*Br}/PVP

The EMP data on the non-brominated Epoxy/PVP interface are compared with those on the brominated Epoxy^{*Br}/PVP interface reported in the previous paper [16] under the same conditions and listed in Table 1.

The second, third, and fourth columns show the results on the Epoxy^{*Br}/PVP prepared at different conditions and the last two columns show the results on the Epoxy/PVP. The results in the third and fourth columns show the effect of molecular weight of PVP. They demonstrate that the interfacial thickness prepared from low-molecular weight PVP was much larger than that prepared from high-molecular weight PVP.

The results in the second and third columns also show that the interdiffusion was controlled by the cure cycle. When the initial cure temperature was chosen to be lower, the interdiffusion was suppressed compared to when it was higher. More importantly, the difference in diffusion front position between DDS and the overall epoxy phase at 0.5 of their normalized concentrations became larger with an increase in the interfacial thickness in the brominated systems. This value shows how close the DDS is located to the PVP phase compared to the overall epoxy. Since the resolution of the EMP was not better than 1.6 μm, as will be shown later, the difference in a diffusion front position of 1 μm would be within the limit of the EMP measurement. However, if the deviation from the stoichiometry between epoxy and DDS becomes significant, it will have important effects on the interphase structure and the properties. For example, the crosslinking of the epoxy at the interphase may be suppressed because of insufficient amounts of curing agent and the not-fully-reacted curing agent in the PVP phase might then act as a plasticizer.

The comparison between the brominated epoxy system and the non-brominated epoxy system under the same cure conditions indicated that the interdiffusion was facilitated in the non-brominated system, resulting in a larger interfacial thickness. Also the difference in the diffusion front position between DDS and epoxy became negligible for the non-brominated epoxy system, but was significant for some brominated epoxy systems.

Thus, there appears to be a clear difference between the non-brominated epoxy and the brominated epoxy at the interface with PVP. The interdiffusion which determines the interface structure would be driven by several factors during the interface formation. For example, the molecular dynamics of each species, thermodynamics described by the Flory–Huggins parameters of the species, $\chi_{DDS\text{-}Epoxy}$, $\chi_{Epoxy\text{-}PVP}$, $\chi_{PVP\text{-}DDS}$, the cure kinetics, and the difference in the net fluxes between two directions at the interface called 'Kirkendall effect' [15]. Since the cure reaction transforms the epoxy structure, most of these factors would be variables during the interface formation.

First, as for the molecular dynamics, Simpson and Bidstrup measured dynamic viscosity and ionic conductivity during the cure reaction between DGEBA and DDS, which characterized chain segment mobility and ion mobility, respectively [19]. During the isothermal cure at 177°C, the viscosity (η) increased rapidly at the initial cure stage; however, it leveled off after ca. 40 min. On the other hand, the ionic conductivity (σ) decreased gradually and leveled

Table 1
Epoxy/PVP and Epoxy^{*Br}/PVP

Epoxy	(1/1 by wt.) DER331/DER542	(1/1 by wt.) DER331/DER542	(1/1 by wt.) DER331/DER542	DER331	DER331
PVP[c]	PVP(K90)	PVP(K90)	PVP(K17)	PVP(K90)	PVP(K90)
Cure conditions					
1st step	130°C (4 h)	170°C (2 h)	170°C (2 h)	130°C (4 h)	170°C (2 h)
2nd step	220°C (1 h)	220°C (1 h)	220°C (1 h)	220°C (1 h)	220°C (1 h)
Interfacial thickness					
Brominated epoxy	12 μm	36 μm[b]	124μm[b]	—	—
DDS	9 μm	12 μm	35 μm	10 μm	22 μm
PVP	9 μm	22 μm	53 μm	13 μm	26 μm
$\Delta Distance_{(DDS\text{-}Epoxy)}$[a]	1 μm	4 μm	9 μm	1 μm	1 μm

[a] Difference in distance between the two species at 0.5 of their normalized concentrations.
[b] The profile was fit to the Weibull distribution function.
[c] M_v of PVP(K17) = 9200, M_v of PVP(K90) = 1 100 000.

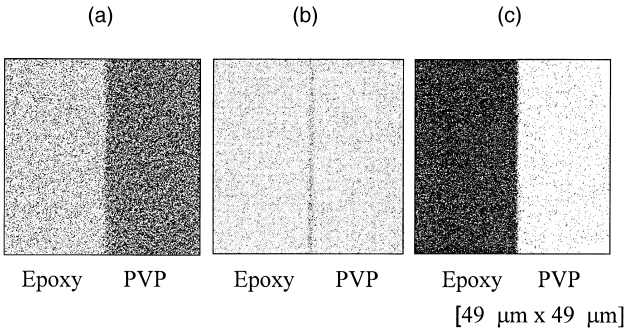

Fig. 10. Interface image of the pre-cured epoxy/PVP bilayer film measured by EMP (49 × 49 μm): (a) monitored by the nitrogen signal; (b) monitored by the gold signal; (c) monitored by the sulfur signal.

off at the latter stage. The results were rationalized by the fact that the ions present in the system (sodium and chloride resulting from the synthesis of DGEBA) were considerably smaller than the mobile chain segments in the epoxy and required less free volume to maintain mobility in the developing network. This illustrates the free volume requirement for the diffusing species. Furthermore, an inverse relationship was observed between η and σ, in which there was no discontinuity at the gel point.

Simpson and Bidstrup also modified the Berry–Fox relationship based on free volume theory [24] to express the temperature dependence of viscosity (η) and ionic conductivity (σ). The model estimated the fractional free volume required for chain segment motion (B), which increased as chain segment growth prior to gelation as:

$$B = 0.361 + 0.00148 \times T_g\ (^{\circ}C)$$

If the gelation occurred at 0.58 of the cure conversion as they reported, it was estimated from their data that *B* corresponded to 0.43 at the gel point. Models based on free volume theory have been extremely successful in describing the temperature and cure dependence of diffusion of polymer chain segments, solvent molecules, or ionic species in polymers [25,26]. Similarly, in our study, the molecular dynamics of each species are probably controlled by the free volume. In other words, the chain development of the epoxy upon a cure reaction will require a larger free volume for diffusion so that the diffusion of the epoxy both in the epoxy bulk and at the interface will be suppressed significantly as the cure reaction progresses.

Furthermore, the brominated epoxy, DER542, contains bulky brominated groups in the structure and a longer chain length than the non-brominated epoxy, DER331, which will require a larger free volume for the diffusion. Thus, the higher diffusivity of the nonbrominated epoxy pre-polymer compared to that of the brominated epoxy might result in a larger interphase and reduce the difference in the diffusion front position between the epoxy and DDS.

Next, the polarity of the bromine groups contributes to make DER542 semi-crystalline at room temperature, even though non-brominated DER331 is a viscous liquid. As for the molecular dynamics of PVP, the PVP bulk was still in a glassy state at the initial cure stage, whereas it was in a rubbery state at the postcure stage, although the initial cure stage had a larger interdiffusion than the postcure stage. This implies that the fast-diffusing species at the initial cure stage, i.e. epoxy, is more dominant over the interdiffusion compared to the slow-diffusing species, i.e. PVP. The contribution of the large change in the molecular dynamics of the epoxy seems to significantly affect the diffusion, in which shorter epoxy chains at the initial cure stage require a much smaller free volume for the diffusion compared to longer chains or crosslinked chains at the latter cure stage.

The polarity of the brominated epoxy might also cause a difference in the interactions at the interface resulting in different $\chi_{\text{DDS-Epoxy}}$ and $\chi_{\text{Epoxy-PVP}}$. Since the chemical structure of the epoxy transforms during the cure, these χ parameters would also be variables. Lastly, it is reported that the brominated epoxy has a much larger cure rate than the non-brominated epoxy with DDS [27]. In other words, the net diffusion time, in which the molecular weight of the epoxy stayed low enough for the epoxy to possess diffusivity, was much shorter for the brominated system than that for the non-brominated epoxy system. This might be a part of the reason that the interfacial thickness in the Epoxy^{*Br}/PVP was smaller than that in the Epoxy/PVP.

3.3. Cured Epoxy/PVP bilayer film

3.3.1. Interface image

In order to confirm that the diffusion at the interface becomes suppressed after the epoxy has formed the network structure, bilayer films of the precured epoxy and PVP were prepared. The epoxy was fully cured first by heating at 170°C (2 h) + 220°C (2 h) in an inert gas atmosphere and then a PVP solution of a methanol/water mixture (1/1 by volume) was cast on top. After the PVP film was dried completely, the resultant bilayer film was heated at the postcure temperature of 220°C for different times.

Fig. 10 shows the interface images of the cured epoxy/PVP bilayer film before heating, as measured by EMP in the mapping mode. During the sample preparation, gold (200 nm thickness) was sputtered on the cured epoxy surface before the PVP was cast. Image (a) was obtained by monitoring the nitrogen signal, image (b) was obtained by measuring the gold signal, and image (c) was obtained from the sulfur signal. The dimensions were set to 49 × 49 μm. The intensity of the color corresponds to the concentration of each element present in the interface region. The nitrogen showed a higher intensity in the PVP phase than in the epoxy phase, and the sulfur showed the opposite result as expected. The gold showed the interface position. These images were again shown without background subtraction because the relative comparison between two phases was sufficient to get normalized concentration profiles at the interface.

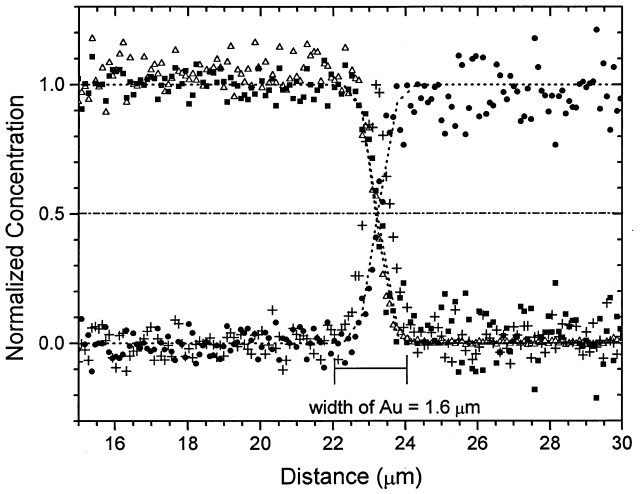

Fig. 11. Normalized concentration profile of the pre-cured epoxy/PVP interface (before the heating). (●) PVP; (△) DDS; (■) Epoxy (calculated); (+) Au.

3.3.2. Analysis of the cured epoxy/PVP interface

Using the interface images shown in Fig. 10, the normalized concentration profiles of the cured epoxy/PVP interface before heating were obtained, as given in Fig. 11. In this figure, the gold marker showed a width of 1.6 μm, even though the real thickness was 0.2 μm. The interfacial thickness of other species, PVP, DDS, and epoxy, was also observed in the same range, even though there was supposed to be no diffusion in this system. This result indicates that the limit of resolution in the EMP under this experimental condition is 1.6 μm.

When the bilayer films of the cured epoxy and PVP were heated at 220°C for different times, the interfacial thickness was of the order of the resolution in electron microprobe analysis, as shown in Fig. 12. The measurements were carried out in the mapping mode. It can be concluded that diffusion was suppressed after the epoxy formed a network structure. If there should be some diffusion at the interface, the extent would be too small to be observed by EMP in this time scale.

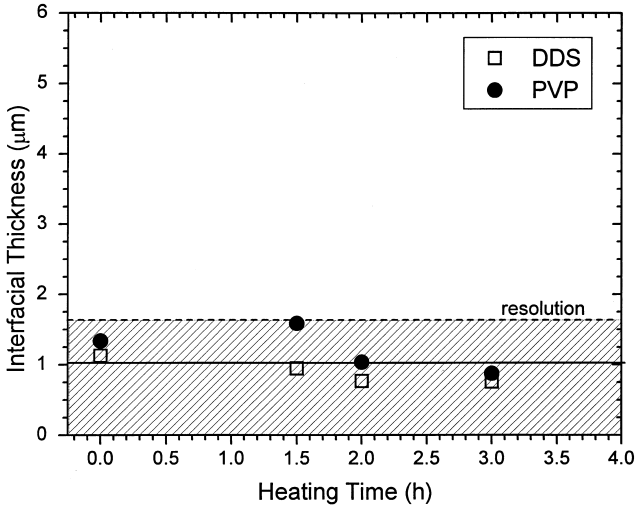

Fig. 12. Interfacial thickness of the pre-cured epoxy/PVP during the heating at 220°C. The resolution was estimated from the gold marker.

In summary, results on three systems have been reported. First, bilayer films of brominated epoxy and PVP (Epoxy^{*Br}/PVP) studied in a previous work; second, bilayer films of non-brominated epoxy and PVP (Epoxy/PVP); and third, bilayer films of the precured epoxy and PVP. Interdiffusion at the interface between PVP and epoxy was controlled by both the molecular weight of PVP and the cure cycle. The stoichiometry between the curing agent and the epoxy was not always preserved at the interphase. The initial cure stage predominantly controlled the interface formation. In the present work, new techniques using EMP were developed to analyze the polymer interface. It was demonstrated that EMP was a powerful tool, which provided not only the concentration profile at the interface but also an image of the interface.

4. Conclusion

The interface structure between thermoplastic PVP and thermoset epoxy resin was investigated by electron microprobe analysis (EMP). The interface formation was controlled by both the molecular weight of PVP and the cure cycle. The stoichiometry between the curing agent and the epoxy was not always preserved in the interphase, implying significant effects on interphase properties. The initial cure stage predominantly controlled the interface formation, whereas the postcure stage had little effect on the interface structure. The present work represents a pioneering study of the thermoplastic/thermoset polymer interface, in which new analytical techniques were developed.

Acknowledgements

This work was supported by the NSF Science and Technology Center for High Performance Polymeric Adhesives and Composites at Virginia Polytechnic Institute and State University under Contract #DMR-9120004. The authors thank Prof. R.J. Tracy and Prof. J.R. Craig in the Department of Geological Sciences for their help with the electron microprobe analysis, Mr. Robert Young and Prof. Don Baird for the help in curing the materials.

References

[1] Wool RP. Polymer interfaces: structure and strength. Munich: Hanser Publisher, 1995.
[2] Wu S. Polymer interfaces and adhesion. New York: Marcel Dekker, 1982.
[3] Kinloch AJ. Adhesion and adhesives, 1st ed. London: Chapman and Hall, 1987.

[4] Gilmore PT, Falabella R, Laurence RL. Macromolecules 1980;13:880.
[5] Spontak RJ, Williams MC, Agard DA. Macromolecules 1988;21:1377.
[6] Kressler J, Higashida N, Inoue T, Heckmann W, Seitz F. Macromolecules 1993;26:2090.
[7] Russell TP, Hjelm Jr. RP, Seeger PA. Macromolecules 1990;23:890.
[8] Valenty SJ, Chera JJ, Olson DR, Webb KK, Smith GA, Katz WJ. J Am Chem Soc 1984;106:6155.
[9] Whitlow SJ, Wool RP. Macromolecules 1989;22:2648.
[10] Jabbari E, Peppas NA. J Mater Sci 1994;29:3969.
[11] Eklind H, Hjertberg T. Macromolecules 1993;26:5844.
[12] Hong PP, Boerio FJ, Clarson SJ, Smith SD. Macromolecules 1991;24:4770.
[13] Tead SF, Kramer EJ, Russell TP, Volksen W. Polymer 1992;33(16):3382.
[14] Kramer EJ. MRS Bull 1996;21:37.
[15] Kramer EJ, Green PF, Palmstrom CJ. Polymer 1984;25:473.
[16] Oyama HT, Wightman JP, Lesko JJ. J Polym Sci, Polym Phys Ed 1997;35:331.
[17] Reed SJB. Electron microprobe analysis, 2nd ed. Cambridge: Cambridge University Press, 1993.
[18] Robinson BV, Sullivan FM, Borzelleca JF, Schwartz SL. PVP; a critical review of the kinetics and toxicology and polyvinylpyrrolidone (Povidone). Lewis Publishers, 1990:14.
[19] Simpson JO, Bidstrup SA. J Polym Sci, Polym Phys Ed 1995;33:55.
[20] Min B-G, Stachurski ZH, Hodgkin JH. Polymer 1993;34:4908.
[21] Min B-G, Stachurski ZH, Hodgkin JH. Polymer 1993;34:4488.
[22] Barton JM. In: Chiu J, editor. Polymer characterization by thermal methods of analysis. New York: Marcel Dekker, 1974.
[23] Crank J. The mathematics of diffusion, 2nd ed. Oxford: Oxford Science Publications, 1975.
[24] Berry GC, Fox TG. Adv Polym Sci 1968;5:261.
[25] Doolittle AK. J Appl Phys 1951;22:1031.
[26] O'Conner KM, Scholsky KM. Polymer 1989;30:461.
[27] Naé HN. J Appl Polym Sci 1987;33:1173.